Scientia Iranica B (2022) 29(6), 3063–3071

SCIENTIA IRANICA

Sharif University of Technology
Scientia Iranica
Transactions B: Mechanical Engineering
http://scientiairanica.sharif.edu

Numerical study on the effect of magnetic field and discrete heating on free convection in a porous container

S. Sivasankaran[a,*], M. Bhuvaneswari[b], and A.K. Alzahrani[a]

a. *Mathematical Modelling and Applied Computation Research Group, Department of Mathematics, King Abdulaziz University, Jeddah, Saudi Arabia.*
b. *Department of Mathematics, Kongunadu Polytechnic College, D. Gudalur, Dindigul, Tamilnadu, India.*

Received 8 September 2021; received in revised form 14 January 2022; accepted 19 September 2022

KEYWORDS
Natural convection;
Inclined magnetic field;
Porous medium;
Discrete heater.

Abstract. A numerical study of buoyancy-induced convection current in a porous container of square shape in the presence of a uniform magnetic flux is conducted. The vertical wall situated on the left side is heated using two discrete heaters, and the constant temperature is maintained on the right side. There is no thermal transfer through the horizontal walls. Brinkman-Forchheimer Darcy-extended model was employed in this study. The non-dimensional leading equations were evaluated using the finite volume method. The effects of different values of the porosity, direction of the magnetic flux, Hartmann number, Rayleigh number, and Darcy number were also evaluated. The results revealed that the Hartmann number and average thermal energy transport were disproportionate to each other as were the average heat transfer and Darcy number.

1. Introduction

The analysis of buoyancy convection current and thermal energy transportation inside a porous channel has gained significance over the last few decades due to their many industrial and technological applications such as water aquifer river, geothermal power stations, exothermal from nuclear reactor, fluidized bed reactors, warehouse of grains, food preservation, and soil toxicity prevention [1–3]. Several studies attempted to examine convection current with thermal energy transportation within porous media as well as the effects of buoyancy convection current in a porous container using partial heating. For instance, Sivasnakaran et al. [4] studied the impacts of disconnected heating on the buoyancy convection current. They observed that the maximum average energy transfer rate was obtained in the heater located at the bottom rather than in the heater located at the top. Beckermann et al. [5] experimentally and numerically studied the steady state buoyancy convection in a rectangular enclosure partially treated with a fluid saturated porous medium. They reported that the fluid penetrating into a porous layer of high permeability could affect the buoyancy convection flow patterns.

Sivshankaran et al. [6] numerically studied the mixed convection in a square-shaped lid-driven cavity with vertical walls of partially heating and cooling functions. Three locations were considered in their study: one parallel and two dissimilar ones. They found that the parallel location maintained higher energy transport than the dissimilar ones. Oztop et al. [7] numerically examined the steady buoyancy convection current in a partially open porous container. They reported that upon increasing the Grashof number, the local thermal energy transportation was enhanced. The

*. *Corresponding author. Tel: +966546649072*
E-mail address: sd.siva@yahoo.com (S. Sivasankaran)

doi: 10.24200/sci.2022.59029.6025

novelty of this study lies in its proposal of methods for inventing a cooling system for electronic components under harmless functioning conditions. Alturaihi et al. [8] examined the impact of porosity from a circular bar with high temperature inside a square porous container. They stated that an increase in the porosity and thermal conductivity ratio would increase the thermal energy transportation rate. Zaho et al. [9] numerically investigated the double diffusive convection current in a porous enclosure with partial heating and salting. Janagi et al. [10] explored the buoyancy convection current in a porous container of square size with sinusoidal heating effects. According to their findings, the average thermal energy transportation rate increased upon increasing the void fraction.

A number of authors have investigated the magneto convection in a closed container with several effects [11–16]. For instance, Çolak et al. [17] investigated the effect of partial heating (40% of length) outcome on Magnetohydrodynamic (MHD) convective current in a driven chamber. They found that the mean Nusselt number in a reverse lid motion increased by 57.2%, compared to that in a positive lid-driven direction. Mondal and Mahapatra [18] explored the effect of discrete heat and mass sources on MHD double-diffusive convection current of nanofluid in a trapezoidal chamber. Roy [19] explored the magneto-convective stream of a hybrid nanofluid in a container with multiple thermal sources in the bottom area. They remarked that the mean Nusselt number increased due to increase in the number of heat sources as well as the angle of magnetic field. Sivasankaran et al. [20] numerically examined the mixed convective current in a lid-driven chamber of square shape encompassing the magnetic field. According to their findings, the magnetic induction affects the stream and energy transfer.

The significance of a magnetic field for the buoyancy convection current in a porous container lies in its applications as in nuclear fuel wastes, freezing of metal alloys, and geothermal reservoirs [21–25]. Khan et al. [21] investigated the combined energy and mass transport in steady MHD flow of viscoelastic fluid with stretching porous walls of a channel. As shown earlier, a rise in the combined parameter value and Reynolds number would consequently increase the temperature and concentration profiles. Chamkha et al. [22] explored the magneto convection inside a porous container. Niranjan et al. [23] took into consideration the Soret Dufour effects and studied the MHD flow of a viscous fluid towards a (vertical) porous plate. They found that an increase in the value of Dufour parameter would increase the temperature and velocity, and the consequent enhancement of chemical reaction parameter would decrease the concentration profiles. Jasim [24] studied the buoyancy convection current inside a cylindrical annulus containing a magnetic flux. He declared that an increase in the magnetic flux would decrease the average Nu. Giwa et al. [25] evaluated the impact of magnetic flux on the buoyancy-driven convection current containing nanofluid. Ghaffarpasand and Fazeli [26] invented the outcome of the magnetic field on the mixed convection of nano-liquid in a non-Darcian porous chamber.

Ahmed and Rashed [27] found that an increase in Hartmann number and a decrease in Darcy number blocked the liquid movement while increasing the heat transfer. Sheikholeslami et al. [28] explored the Electrohydrodynamics (EHD) radiative convective current of nano-liquid in a porous chamber. They found that convection declined with a rise in Hartmann number. Bég et al. [29] inspected the MHD Marangoni-convection in a Darcy porous rectangular chamber with internal temperature generation. Ali et al. [30] explored the MHD (mixed) heat transfer of (Cu-water) nanoliquid in a trapezoidal porous container due to a circular solid cylinder. They observed that the averaged Nu number declined by about 90% when the cylinder rotated in a counter-clockwise way and Ri increased. In their study on the MHD flow of hybrid nanofluid in an elliptic porous space, Shehzad et al. [31] found that Nu declined due to the unfavorable effect of the MHD. Al-Farhany et al. [32] scrutinized the MHD convective current in a nanofluid soaked porous tilted chamber. They observed that the averaged Nusselt number increased upon increasing the Darcy number and fins length. Dogonchi et al. [33] studied the MHD convection of hybrid nanoliquid in a porous wavy cavity. Abderrahmane et al. [34] explored the MHD convection stream of non-Newtonian nanoliquid in a halved annulus porous enclosed area. They remarked that the magnetic field suppressed the velocity; hence, Nusselt number diminished.

Several studies have addressed natural convection in porous containers in the absence of a magnetic field in the literature. In most of these studies, either isothermally heated wall or partially heated wall is considered as the heating source. However, in many electronic equipment, thermal sources are distributed in more than one place. Any study on the convective flow in containers with discrete thermal sources has not been extensively investigated. Therefore, to fill this gap, the present study investigated the buoyancy-induced magnetic-convection effect using dual distinct heaters in the left wall of the square porous container with a magnetic force imposed in different directions.

2. Mathematical formulation

The laminar, unsteady and buoyancy convective flow and thermal energy transport inside a container of size D were loaded with a void fraction fluid medium, as represented in Figure 1. The boundary values and

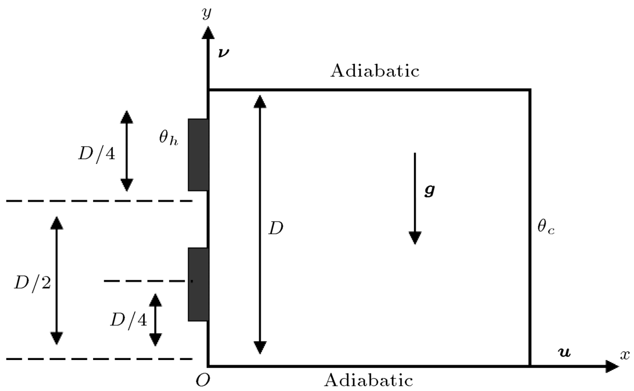

Figure 1. Physical Model and coordinate systems.

coordinate settings are diagrammatically represented in Figure 1. A pair of heaters of size $D/4$ (limited in size) were placed on the left wall and simultaneously, the non-thermal portion of the left wall was covered from heat. The right wall of the container receives constant temperature distribution, and heat is restricted at the top and bottom walls. The liquid in the vacant space is dense in nature. The gravitational force is exerted in the vertically downward direction. The horizontal and vertical velocity components are u and v, respectively. The Brinkman Forchheimer-Darcy extended model was employed, and the homogeneous, isotropic porous container was maintained in this study. The liquid and porous container were kept at a thermodynamic equilibrium position. Apart from density in terms of buoyancy, the thermal properties of the fluid remained the same. The density was linearly modified by the temperature as $\rho = [1 - \beta(\theta - \theta_0)]\rho_0$, where β represents the thermal expansion coefficient and subscript 0 denotes the reference state. For further calculation, Boussinesq approximation was used.

Inside the cavity, electrically charged fluid with small Prandtl number is taken into consideration. An unvarying magnetism is applied with a constant magnitude B_0. The variables $F = \sigma_\varepsilon(V \times B) \times B$ and $J = \sigma_\varepsilon(V \times B)$ represent the electromagnetic force F and electric current J, respectively. The induced magnetic field owing to the movement of the electrically conducting liquid is (very) small compared to the applied magnetic field. An angle $\tan\phi = B_y/B_x$ is the angle between the horizontal axis and magnetic field. Of note, negligible viscous dissipation was also considered in this study. Based on the aforementioned assumptions, the leading equations can be written as follows:

$$\frac{\partial u}{\partial x} + \frac{\partial v}{\partial y} = 0,$$

$$\frac{1}{\varepsilon}\frac{\partial u}{\partial t} + \frac{1}{\varepsilon^2}\left[u\frac{\partial u}{\partial x} + v\frac{\partial u}{\partial y}\right] = -\frac{1}{\rho_0}\frac{\partial p}{\partial x} \tag{1}$$

$$+\frac{v}{\varepsilon}\left[\frac{\partial^2 u}{\partial x^2} + \frac{\partial^2 u}{\partial y^2}\right] - \frac{v}{K}u - \frac{Fc}{\sqrt{K}}u\sqrt{u^2+v^2}$$

$$+\frac{\sigma_\varepsilon B_0^2}{\rho_0}(v\sin\phi\cos\phi - u\sin^2\phi), \tag{2}$$

$$\frac{1}{\varepsilon}\frac{\partial v}{\partial t} + \frac{1}{\varepsilon^2}\left[u\frac{\partial v}{\partial x} + v\frac{\partial v}{\partial y}\right] = -\frac{1}{\rho_0}\frac{\partial p}{\partial y}$$

$$+\frac{v}{\varepsilon}\left[\frac{\partial^2 v}{\partial x^2} + \frac{\partial^2 v}{\partial y^2}\right] - \frac{v}{K}v - \frac{Fc}{\sqrt{K}}v\sqrt{u^2+v^2}$$

$$+g\beta(\theta-\theta_0) + \frac{\sigma_\varepsilon B_0^2}{\rho_0}(u\sin\phi\cos\phi - v\cos^2\phi), \tag{3}$$

$$\sigma\frac{\partial \theta}{\partial t} + u\frac{\partial \theta}{\partial x} + v\frac{\partial \theta}{\partial y} = \frac{k}{\rho_0 c_p}\left(\frac{\partial^2\theta}{\partial x^2} + \frac{\partial^2\theta}{\partial y^2}\right), \tag{4}$$

where $Fc = \frac{1.75}{\sqrt{150\varepsilon^{3/2}}}$ and t, p, θ, β, K, K, v, ρ_0, σ, c_p, k, ε , and g denote the time, pressure, temperature, volumetric coefficient of thermal expansion, permeability of the porous medium, kinematic viscosity, density, specific heat ratio, specific heat, heat conduction, porosity of the medium, and gravitational acceleration, respectively. The suitable preliminary and edge conditions are:

$$t = 0: \ v = u = 0, \ \ \theta = 0, \ \ 0 \le y \le D, \ \ 0 \le x \le D,$$

$$t > 0: \ v = u = 0, \ \ \frac{\partial\theta}{\partial y} = 0, \ \ y = D\&0,$$

$$x = 0:$$

$$v = u = 0, \ \theta = \theta_h \quad \text{on heaters;}$$

$$\frac{\partial\theta}{\partial x} = 0, \quad \text{elsewhere;}$$

$$x = L:$$

$$v = u = 0, \ \ \theta = \theta_0. \tag{5}$$

The leading equations are non-dimensionalized by the following variables:

$$X = \frac{x}{D}, \ Y = \frac{y}{D}, \ U = \frac{uD}{v}, \ V = \frac{vD}{v}, \ T = \frac{\theta - \theta_t}{\theta_h - \theta_t},$$

$$\tau = \frac{tv}{D^2}, \ \ p = \frac{pD^2}{\rho_0 v^2}. \tag{6}$$

The resulting dimensionless identities are:

$$\frac{\partial U}{\partial X} + \frac{\partial V}{\partial Y} = 0, \tag{7}$$

$$\frac{1}{\varepsilon}\frac{\partial U}{\partial \tau} + \frac{1}{\varepsilon^2}\left[U\frac{\partial U}{\partial X} + V\frac{\partial U}{\partial Y}\right] = -\frac{\partial P}{\partial X} + \frac{1}{\varepsilon}\nabla^2 U$$

$$-\frac{U}{Da}-\frac{Fc}{\sqrt{Da}}U\sqrt{U^2+V^2}$$
$$+Ha^2(V\sin\phi\cos\phi-U\sin^2\phi), \qquad (8)$$

$$\frac{1}{\varepsilon}\frac{\partial V}{\partial \tau}+\frac{1}{\varepsilon^2}\left[U\frac{\partial V}{\partial X}+V\frac{\partial V}{\partial Y}\right]=-\frac{\partial P}{\partial Y}+\frac{1}{\varepsilon}\nabla^2 V$$
$$-\frac{V}{Da}-\frac{Fc}{\sqrt{Da}}U\sqrt{U^2+V^2}$$
$$+\frac{Ra}{Pr}T+Ha^2(V\sin\phi\cos\phi-U\sin^2\phi), \qquad (9)$$

$$\frac{\partial T}{\partial \tau}=\frac{1}{Pr}\nabla^2 T-U\frac{\partial T}{\partial X}-V\frac{\partial T}{\partial Y}. \qquad (10)$$

The non-dimensional parameters involved in the previous identities are $Da = K/D^2$, Darcy number, $Ra = \frac{g\beta(\theta_h-\theta_t)D^3}{va}$, Rayleigh number, $Ha = B_0D\sqrt{\sigma_\varepsilon/\mu}$, Hartmann number, and $Pr = v/\alpha$, Prandtl number.

The boundary and initial conditions (dimensionless form) are:

$$\tau=0: \quad V=U=0, \quad T=0 \quad 0\leq Y\leq 1, \quad 0\leq X\leq 1$$

$$\tau>0: \quad V=U=0, \quad \frac{\partial T}{\partial Y}=0 \quad Y=1\&0$$

$$x=0:$$

$$V=U=0, \; T=1 \;\text{ on heaters;}$$

$$\frac{\partial T}{\partial X}=0 \;\text{ elsewhere;}$$

$$x=1:$$

$$V=U=0, \quad T=0. \qquad (11)$$

The thermal energy transportation rate across the container is a significant parameter in the thermal energy transfer system. The local Nusselt number along the heaters and the right vertical wall of the container are defined as $Nu_h = \left(-\frac{\partial T}{\partial X}\right)$ and $Nu_c = \left(-\frac{\partial T}{\partial X}\right)_{X=1}$, respectively. The total thermal energy transport rate across the container is the sum of the mean Nusselt numbers along the heaters. The mean Nusselt numbers along the heaters are stated as:

$$\overline{Nu}=\int\limits_{\text{heater 1}} Nu_h dY+\int\limits_{\text{heater 2}} Nu_h dY.$$

3. Numerical technique and validation

The finite volume was employed to solve the non-dimensional Eqs. (7)–(10) related to the boundary condition (11) with SIMPLE algorithm for pressure-velocity coupling. The leading equations were transformed into an algebraic system of equations and, then, solved iteratively. A non-uniform grid was chosen in each of these particular directions to cluster the grid points just across from the external wall. To ensure that the outcomes are grid-size autonomous, different grid sizes were evaluated from 41×41 to 161×161 for $Ra = 10^6$ and $Pr = 0.71$. Owing to the performance and computational period, the grid independence experiment on a 121×121 non-uniform grid proved to be sufficient to start investigating this model. The (mean) Nusselt number was estimated using Simpson's (1/3) rule. The convergence condition used for the field variables $\varphi(=T,V,U)$ is $\left|\frac{\varphi_{(m+1)}(i,j)-\varphi_m(i,j)}{\varphi_{(m+1)}(i,j)}\right| \leq 10^{-6}$. The subscript m denotes the preceding estimate at the iteration and $m+1$ denotes the current estimate.

In a numerical study, validation of a computer code is critical. For the possible solution in question, an in-house numerical code was created. A test case was also employed to verify the accuracy of the computer code in this study. The validity of the current computational code in the reported methods as well as natural convection in a porosity membrane was checked [2], the results of which are given in Table 1. According to the findings, there is a correlation between some of the current and previous findings, thus confirming the reliability of the current code for studying the problem at hand.

Table 1. Comparison of $\overline{Nu}$ for free convection in a porous container with $\varepsilon = 0.4$ and $Pr = 1.0$

		$\overline{Nu}$	
Da	**Ra**	**Nithiarasu et al. [2]**	**Present**
10^4	10^5	1.067	1.074
	10^6	2.550	2.688
10^{-2}	10^3	1.010	1.007
	10^4	1.408	1.343
	10^5	2.983	2.993

4. Results and discussion

A mathematical simulation was executed to elaborate the convection current, and the thermal pattern with a penetrable container and a uniform external magnetic field was found to be quite present inside the container with two discrete thermal sources. The constraints associated with this study are Rayleigh number ($10^3 \leq Ra \leq 10^6$), porosity ($0.1 \leq \varepsilon \leq 0.7$), Darcy number ($10^{-5} \leq Da \leq 10^{-1}$), Hartmann number ($0 \leq Ha \leq 100$), and magnetic field direction ($\phi = 0, 45, 90$). Figure 2 shows the flow behavior and thermal pattern inside the container for different values of Da with $\varepsilon = 0.4, Ha = 50, Ra = 10^6$, and $\phi = 0$. Of note,

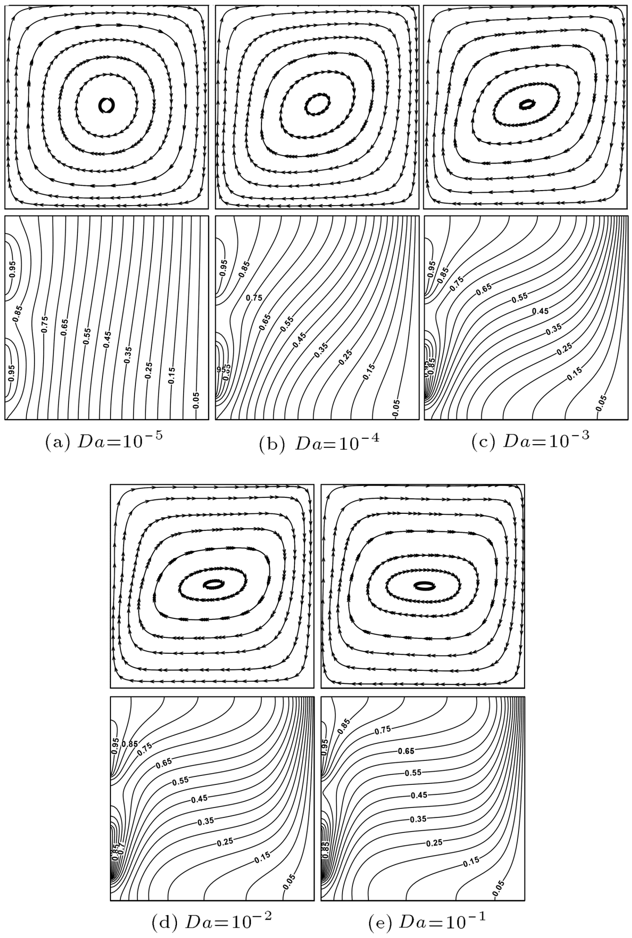

Figure 2. Streamlines (up) and isotherms (down) for different Darcy numbers with $\phi = 0$, Ha= 50, $\varepsilon = 0.4$ and $Ra = 10^6$.

at every value of Da, a single clockwise rotating cell would appear. The shape of the central area of the cell depends upon the values of Da. The circular shape of the core region exists when $Da = 10^{-5}$. Upon an increase in Darcy number, the core region is elongated diagonally first and, then, transformed into a horizontal elliptical shape as a result of increasing the fluid velocity. The corresponding isotherms clearly indicate heat distribution. From the vertical lines of isotherms, it is clearly identified that the conduction type of thermal energy transportation exists when $Da = 10^{-5}$. No thermal boundary layer was observed to be in line with the isothermal walls. Upon increasing the values of Da, the convection mode of thermal energy transportation begins and strong convection occurs at $Da = 10^{-5}$. The thermal boundary layers at the right-top portion of the (cold) wall exist along the heat sources.

Figure 3 presents the flow scheme at different values of Ha and direction of the magnetic flux with $Ra = 10^6$, $Da = 0.001$ and $\varepsilon = 0.4$. In the magnetic flux direction, there is no such noteworthy impact on the flow field at small values of Ha. At the moderate

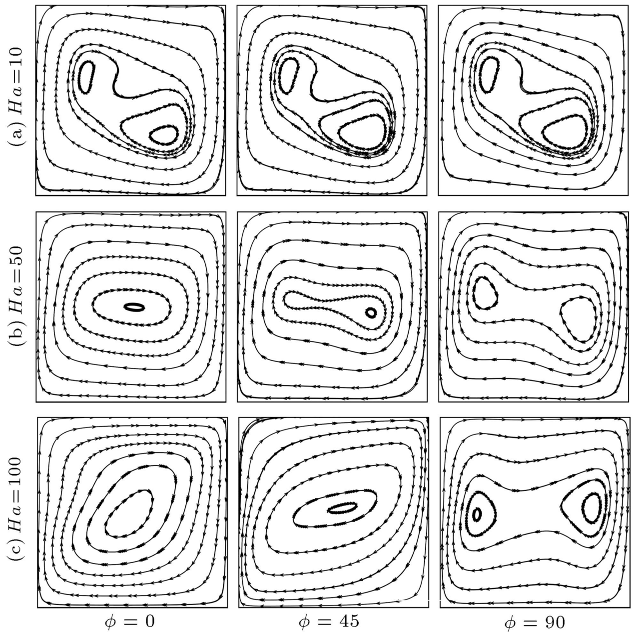

Figure 3. Streamlinesfor different Hartmann number and ϕ for $Ra = 10^6$, $Da = 0.001$ and $\varepsilon = 0.4$

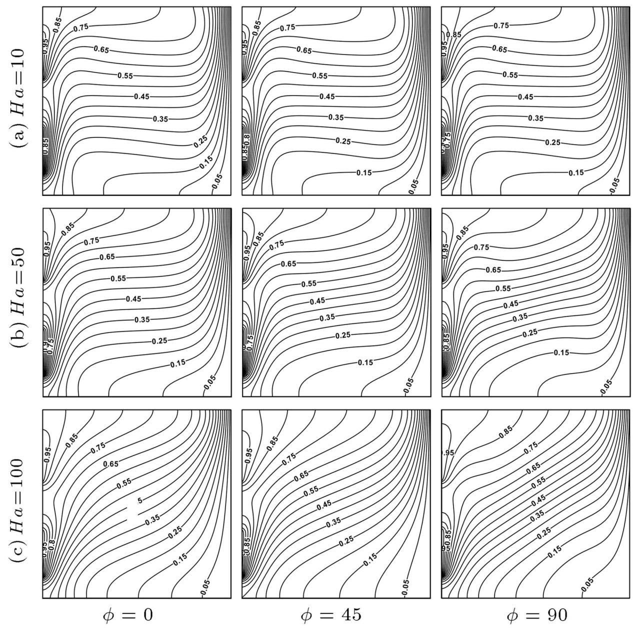

Figure 4. Isotherms for different Hartmann number and ϕ for $Ra = 10^6$, $Da = 0.001$ and $\varepsilon = 0.1$

and high values of $Ha(Ha = 50, 100)$, the magnetic flux direction caused a drastic change in the flow pattern. At $Ha = 100$ the single clockwise rotating eddy elongates in the vertical direction for $\phi = 0°$. The eddy stretches diagonally when $\phi = 45°$, while it stretches horizontally at $\phi = 90°$. The resulting isotherms are shown in Figure 4. The direction of the magnetic field did not have any substantial impact on the thermal distribution. In the case of $Ha = 0$, the vertical temperature stratification was observed at

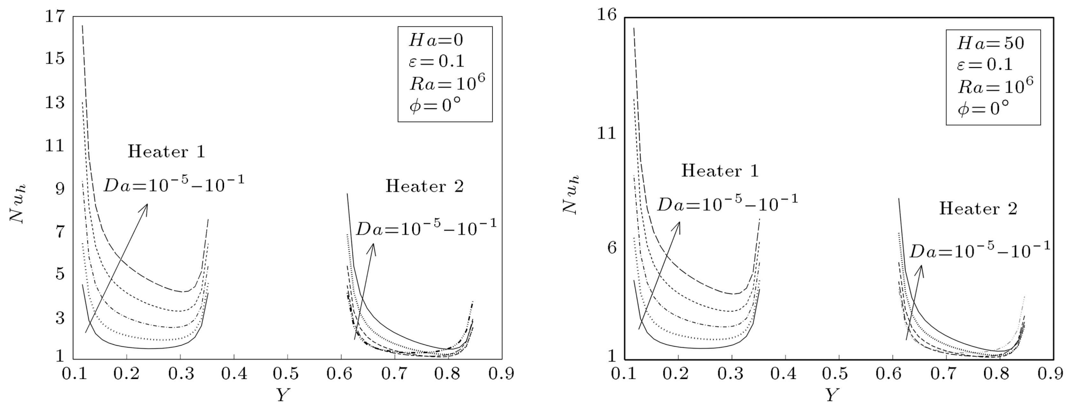

(a) $Ha = 0$ (b) $Ha = 50$

Figure 5. Local Nusselt number along heaters for different Darcy numbers

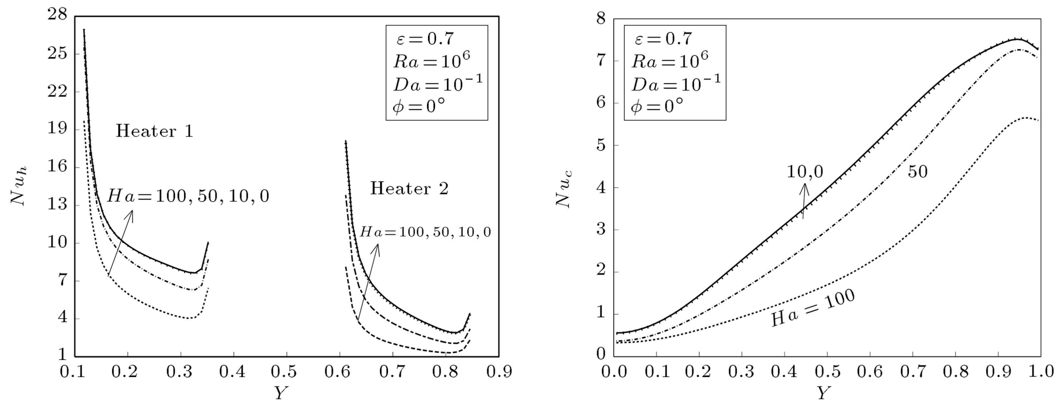

(a) Nu_h (b) Nu_c

Figure 6. Local Nusselt number for different Hartmann numbers

every value of ϕ. In addition, thermal boundary layers are located along the heaters and cold wall . The rise of the magnetic flux strength weakened the thermal boundary. The temperature stratification disappears vertically at $Ha = 100$.

In order to quantify the energy transport at heaters, the local Nu is depicted against the pertinent factors considered in this study. Figures 5 and 6 show the Local Nu for different values of Da and Ha. The local Nu increased with an increase in Darcy number along both heaters. However, Nu_{local} decreases upon increasing the values of Ha. At both edges of the heaters, the local heat transfer is overshoot. However, Nu_{local} is enhanced at the training edge of the heater. Figure 6(b) shows the local thermal energy transportation rate along the cold wall. The high value of local thermal energy transportation rate is noticed at the upper part of the cold wall. Figure 7 presents the time history (transient behaviour) of Nu_{average} at distinct values of Da. At $Da = 10^{-5}$, a longer time period is required to reach a steady state, while a shorter time period is required for $Da = 10^{-1}$. Three folds of time are also required to get the convergence for lower values of Da ($Da = 10^{-5}$), when comparing

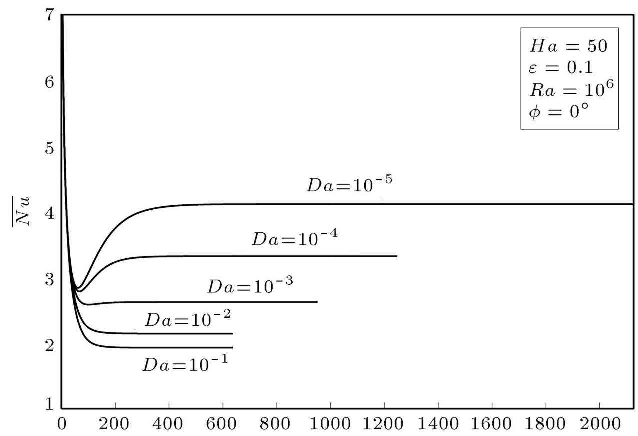

Figure 7. Time history of averaged Nusselt number for different Darcy numbers

the convergence for higher values of Da ($Da = 10^{-1}$).

Figures 8 and 9 show the impact of Nu_{average} on different parameters (Da, ε, Ha and Ra). An increase in Darcy number, porosity, and Rayleigh number would lead to an increase in the Nu_{average} rate. However, Nu_{average} rate declines upon increasing the values of Ha. The non-linear behavior was noticed between

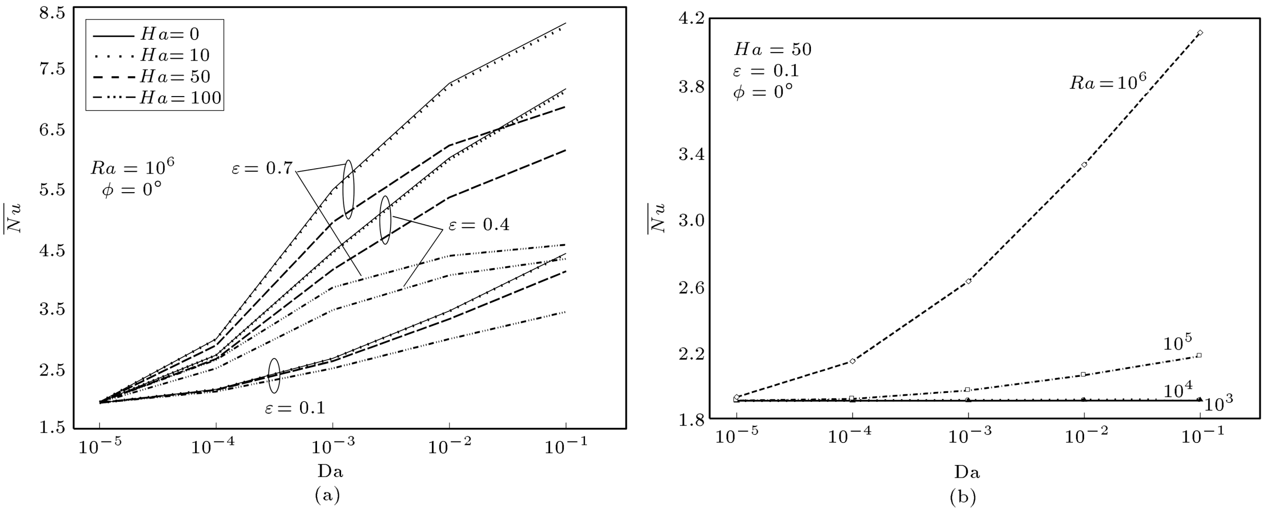

Figure 8. Averaged Nusselt number vs. Darcy number for different Ha, Ra, and porosities

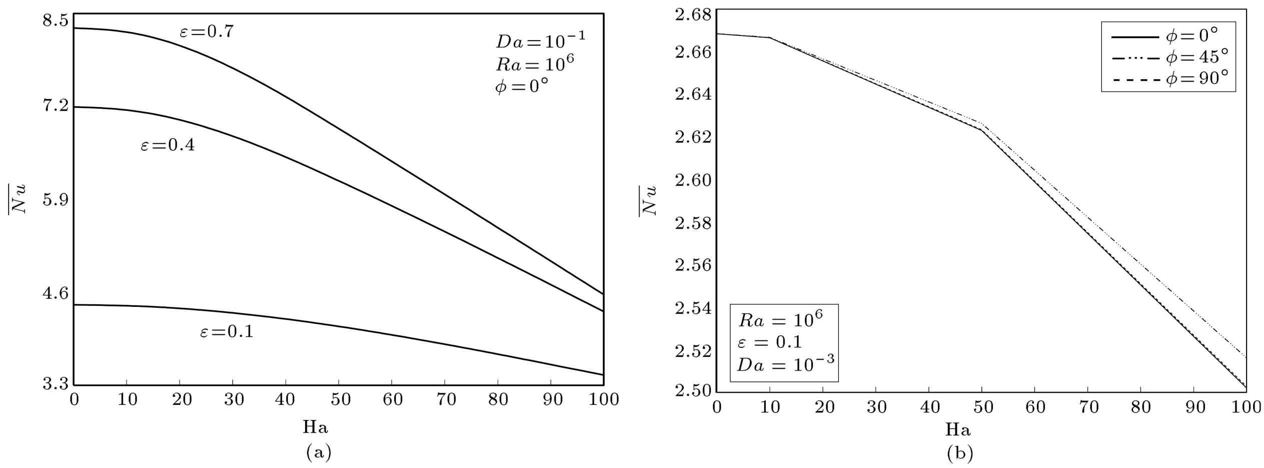

Figure 9. Average Nusselt number vs. Hartmann number for different porosities (a) and magnetic field direction (b).

Nu_{average} and Da. The average heat transport does not change upon changing the values of porosity at $Da = 10^{-5}$. A similar trend holds for changing the values of Ra at $Da = 10^{-5}$. The thermal energy transportation rate is nearly constant for all values of Da as well as minimal values of Ra ($Ra = 10^3$ and 10^4). Figure 9(a) and (b) show the impact of porosity and magnetic field direction at distinct values of Ha. The value of $Nu_{average}$ increases upon enhancing the porosity. On the contrary, $Nu_{average}$ declines with an improvement in the values of Ha. When considering the magnetic flux direction, the vertical direction of magnetic flux offers an enhanced thermal energy transportation rate in comparison to other directions.

5. Conclusion

This study investigated the impact of MHD convective flow and thermal energy transportation in a porous container with two discrete heaters using finite volume technique. The direction of the magnetic field was also examined. The concluding remarks are summarized in the following:

1. The magnetic flux direction had a more significant impact on the fluid flow than that on the heat transfer;
2. Thermal stratification in the vertical direction was observed at small values of Ha;
3. The average thermal energy transportation rate was enhanced upon increasing the values of Da, porosity, and Rayleigh number;
4. The average thermal energy transportation rate decreased with an increase in the Ha value;
5. The value of Nu_{local} reached its maximum at the edges of heater as well as on top of the cold wall;

Acknowledgement

This project was funded by the Deanship of Scientific Research (DSR), King Abdulaziz University, Jeddah, Saudi Arabia, under Grant No. (G-225-130-1441). The authors, therefore, acknowledge, with thanks, the DSR technical and financial supports.

References

1. Walker, K.L. and Homsy, G.M. "Convection in a porous cavity", *J. of Fluid Mech.*, **87**(3), pp. 449–474 (1978).
2. Nithiarasu, P., Seetharamu, K.N., and Sundararajan, T. "Natural convective heat transfer in a fluid saturated variable porosity medium", *Int. J. of Heat and Mass Transfer*, **40**, pp. 3955–3967 (1997).
3. Sankar, M., Bhuvaneswari, M., Sivasankaran, S., et al. "Buoyancy induced convection in a porous cavity with partially thermally active side walls", *Int. J. of Heat and Mass Transfer*, **54**, pp. 5173–5182 (2011).
4. Sivasankaran, S., Do, Y., and Sankar, M. "Effect of discrete heating on natural convection in a rectangular porous enclosure", *Transport in Porous Media*, **86**, pp. 291–311 (2011).
5. Beckermann, C., Ramadhyani, S., and Viskanta, R. "Natural convection flow and heat transfer between a fluid layer and a porous layer inside a rectangular enclosure", *ASME J. of Heat Transfer*, **109**, pp. 363–370 (1987).
6. Sivasankaran, S., Malleswaran, A., Bhuvaneswari, M., et al. "Hydro-magnetic mixed convection in a lid-driven cavity with partially thermally active walls", *Sci. Iran. Trans. Mech. Eng. B*, **24**(1), pp. 153–163 (2017).
7. Oztop, H.F., Al-Salem, K., Varol, Y., et al. "Natural convection heat transfer in a partially opened cavity filled with porous media", *Int. J. of Heat and Mass Transfer*, **54**, pp. 2253–2261 (2011).
8. Alturaihi, M.H., Jassim, L., Alguboori, A.R., et al. "Porosity influence on natural convection heat transfer from a circular cylinder in a square porous enclosure", *J. Mech. Engg. Research and Developments*, **43**, pp. 236–254 (2020).
9. Zhao, F.Y., Liu, D., and Tang G.F. "Natural convection in a porous enclosure with a partial heating and salting element", *Int. J. of Therm. Sci.*, **47**, pp. 569–583 (2008).
10. Janagi, K., Sivasankaran, S., Bhuvaneswari, M., et al. "Numerical study on free convection of cold water in a square porous cavity heated with sinusoidal wall temperature", *Int. J. of Numerical Methods for Heat & Fluid Flow*, **27**(4), pp. 1000–1014 (2017).
11. Shahzad, F., Sagheer, M., and Hussain, S. "Transport of MHD nanofluid in a stratified medium containing gyrotactic microorganisms due to a stretching sheet", *Scientia Iranica: Trans. on Mech. Eng. B*, **28**(6), pp. 3786–3805 (2022).
12. Sivasankaran, S. and Ho, C.J. "Effect of temperature dependent properties on MHD convection of water near its density maximum in a cavity", *Int. J. of Therm. Sci.*, **47**, pp. 1184–1194 (2008).
13. Afsar Khan, A., Batool, R., Kousar, N. "Examining the behavior of MHD micropolar fluid over curved stretching surface based on the modified Fourier law", *Scientia Iranica: Trans. on Mech. Eng. B*, **28**(1), pp. 223–230 (2021).
14. Sivasankaran, S. and Bhuvaneswari, M. "Effect of thermally active zones and direction of magnetic field on hydromagnetic convection in an enclosure", *Therm. Sci.*, **15**(2), pp. S367–S382 (2011).
15. Bhuvaneswari, M., Sivasankaran, S. and Kim, Y.J. "Magneto convection in a square enclosure with sinusoidal temperature distributions on both side walls", *Numer. Heat Transfer, A*, **59**, pp. 167–184 (2011).
16. Sivasankaran, S., Malleswaran, A., Lee, J., et al. "Hydro-magnetic combined convection in a lid-driven cavity with sinusoidal boundary conditions on both sidewalls", *Int. J. of Heat and Mass Transfer*, **54**, pp. 512–525 (2011).
17. Çolak, E., Öztop, H.F., and Ekici, Ö. "MHD mixed convection in a chamfered lid-driven cavity with partial heating", *Int. J. of Heat and Mass Transfer*, **156**, 119901 (2020).
18. Mondal, P. and Mahapatra, T.R. "MHD double-diffusive mixed convection and entropy generation of nanofluid in a trapezoidal cavity", *Int. J. of Mech. Sci.*, **208**, 106665 (2021).
19. Roy, N.C. "MHD natural convection of a hybrid nanofluid in an enclosure with multiple heat sources", *Alexandria Engrg. J.*, **61**(2), pp. 1679–1694 (2022).
20. Sivasankaran, S., Anandhan, S.S., and Hakeem, A.A.K. "Mixed convection in a lid-driven cavity with sinusoidal boundary temperature at the bottom wall in the presence of magnetic field", *Sci. Iran. Trans. on Mech. Eng. B*, **23**(3), pp. 1027–1036 (2016).
21. Khan, S.U., Ali, N., Shehzad, S.A., et al. "Analysis of the second-grade fluid flow in a porous channel by Cattaneo-Christov and generalized Fick's theories", *Sci. Iran, Trans. on Mech. Eng. B*, **27**(4), pp. 1945–1954 (2020).
22. Chamkha, A.J., Mansour, M.A., Rashad, A.M., et al. "Magnetohydrodynamic mixed convection and entropy analysis of nanofluid in gamma-shaped porous cavity", *J. of Thermophysics and Heat Transfer*, **34**(10), pp. 1–12 (2020).
23. Niranjan, H., Sivashankaran, S., and Bhuvaneswari, M. "Chemical reaction, Soret and Dufour effects on MHD convection stagnation point flow with radiation and slip condition", *Sci. Iran, Trans. on Mech. Eng. B.*, **24**(2), pp. 698–706 (2017).
24. Jasim, L.M. "Numerical investigation of the magnetic field effects on natural convection within a porous horizontal cylindrical annulus", *J. Porous Media*, **24**(2), pp. 13–27 (2021).
25. Giwa S.O., Sharifpur, M., Ahmadi, M.H., et al. "A review of magnetic field influence on natural convection heat transfer performance of nanofluids in square cavities", *J. of Thermal Anal. and Calorimetry*, **145**, pp. 2581–2623 (2021).

26. Ghaffarpasand, O. and Fazeli, D. "Numerical analysis of MHD mixed convection flow in a parallelogramic porous enclosure filled with nanofluid and in presence of magnetic field induction", *Scientia Iranica: Trans. on Mech. Eng. B*, **25**(3), pp. 1789-0-180 (2018).
27. Ahmed, S.E. and Rashed, Z.Z. "MHD natural convection in a heat generating porous medium-filled wavy enclosures using Buongiorno's nanofluid model", *Case Studies in Thermal Eng.*, **14**, 100430 (2019).
28. Sheikholeslami, M., Ganji, D.D., Li, Z., et al. "Numerical simulation of thermal radiative heat transfer effects on Fe_3O_4−ethylene glycol nanofluid EHD flow in a porous enclosure", *Scientia Iranica: Trans. on Mech. Eng. B*, **26**(3), pp. 1405–1414 (2019).
29. Bég, O.A., Venkatadri, K., Ramachandra Prasad, V., et al. "Numerical simulation of hydromagnetic Marangoni convection flow in a Darcian porous semiconductor melt enclosure with buoyancy and heat generation effects", *Materials Sci. and Engrg: B*, **261**, 114722 (2020).
30. Ali, F.H., Hamzah, H.K., Hussein, A.K., et al. "MHD mixed convection due to a rotating circular cylinder in a trapezoidal enclosure filled with a nanofluid saturated with a porous media", *Int. J. of Mech. Sci.*, **181**(1), 105688 (2020).
31. Shehzad, S.A., Sheikholeslami, M., Ambreen, T., et al. "Convective MHD flow of hybrid-nanofluid within an elliptic porous enclosure", *Physics Letters A*, **384**(28), 126727 (2020).
32. Al-Farhany, K., Al-Chlaihawi, K.K., Al-dawody, M.F., et al. "Effects of fins on magnetohydrodynamic conjugate natural convection in a nanofluid-saturated porous inclined enclosure", *Int. Commun. in Heat and Mass Transfer*, **126**, 105413 (2021).
33. Dogonchi, A.S., Tayebi, T., Karimi, N., et al. "Thermal-natural convection and entropy production behavior of hybrid nanoliquid flow under the effects of magnetic field through a porous wavy cavity embodies three circular cylinders", *J. of the Taiwan Institute of Chemical Engineers*, **124**, pp. 162–173 (2021).
34. Abderrahmane, A., Hatami, M., Medebber, M.A., et al. "Non-Newtonian nanofluid natural convective heat transfer in an inclined half-annulus porous enclosure using FEM", *Alexandria Eng. J.*, **61**(7), pp. 5441–5453 (2022).

Biography

Sivanandam Sivasankaran received his MSc, MPhil, and PhD degrees from Bharathiar University, India. Then, he received his Post-Doctoral Fellowship at National Cheng Kung University, Taiwan and National Taiwan University, Taiwan. He worked as a Research Professor at Yonsei University, South Korea; an Assistant Professor at Sungkyunkwan University, South Korea; and Senior Lecturer at the Institute of Mathematical Sciences, University of Malaya, Malaysia. He is currently working at King Abdulaziz University, Saudi Arabia. He is an editorial board member in several international journals and a reviewer of more than 60 international journals. He is an Associate Editor in two journals and an academic editor in a journal. He has more than 150 research publications. His areas of interest are convective heat and mass transfer, CFD, nanofluids, micro-channel heat sinks, and porous media.

Marimuthu Bhuvaneswari received her MSc, MPhil, and PhD degrees from Bharathiar University, Coimbatore, India. She received the Post-Doctoral Fellowship twice from National Cheng Kung University, Taiwan and twice from Sungkyunkwan University, South Korea. Then, she worked as a research fellow at University of Malaya, Malaysia. Her research interests are numerical and analytical methods for PDE, boundary layer flow, radiation, and heat and mass Transfer.

Abdullah Khames Alzahrani received his MSc and PhD degrees from Heriot Watt University, UK. He has been working at King Abdulaziz University since 2014. His research interests include application of mathematics to problems in ecology, biology, and physics as well as industrial applied mathematics and numerical analysis for partial differential equations.